

Phenomenological study of the isovector tensor meson family

Cheng-Qun Pang^{1,2,*}, Li-Ping He^{1,2,†}, Xiang Liu^{1,2,‡,§} and Takayuki Matsuki^{3¶}

¹*School of Physical Science and Technology, Lanzhou University, Lanzhou 730000, China*

²*Research Center for Hadron and CSR Physics, Lanzhou University & Institute of Modern Physics of CAS, Lanzhou 730000, China*

³*Tokyo Kasei University, 1-18-1 Kaga, Itabashi, Tokyo 173-8602, Japan*

In this work, we study all the observed a_2 states and group them into the a_2 meson family, where their total and two-body Okubo-Zweig-Iizuka allowed strong decay partial widths are calculated via the quark pair creation model. Taking into account the present experimental data, we further give the corresponding phenomenological analysis, which is valuable to test whether each a_2 state can be assigned into the a_2 meson family. What is more important is that the prediction of their decay behaviors will be helpful for future experimental study of the a_2 states.

PACS numbers: 14.40.Be, 12.38.Lg, 13.25.Jx

I. INTRODUCTION

Among the observed light hadrons, isovector tensor mesons form the a_2 meson family, which has the quantum number $I^G J^{PC} = 1^- 2^{++}$. In Particle Data Group (PDG) [1], seven a_2 states are collected, i.e., $a_2(1320)$, $a_2(1700)$, $a_2(1950)$, $a_2(1990)$, $a_2(2030)$, $a_2(2175)$, and $a_2(2255)$. Here, their experimental information including the resonance parameters and the observed decay channels, is given in Table I.

$a_2(1320)$ can be well established to be the 1^3P_2 state [4, 5] which is the ground state of the a_2 meson family, while $a_2(1700)$ is the first radial excitation of $a_2(1320)$ [6–10]. As shown in Table I, there are five a_2 states listed as further states in PDG. $a_2(1950)$ was observed in the $\pi f_2(1270)$ decay channel by SPEC [2] when fitting it with the Crystal Barrel data. In addition, $a_2(1950)$ was also observed in the process $p\bar{p} \rightarrow \eta\eta\pi$ [11]. Anisovich *et al.* indicated that there exists $a_2(1990)$ [or named $a_2(1980)$] in the reactions $p\bar{p} \rightarrow \pi\eta$, $p\bar{p} \rightarrow \pi\eta'$ [12]. Furthermore, in an analysis combined with the consistent resonance parameters in all three sets of data, ($p\bar{p} \rightarrow \pi\eta$, $\pi\eta'$, 3π), the authors in Ref. [2] updated their analyzed results, in which the former resonances $a_2(1990)$, $a_2(2270)$ [12], $a_2(2100)$, and $a_2(2280)$ [12] are replaced with $a_2(1950)$, $a_2(2030)$, $a_2(2175)$, and $a_2(2255)$. Thus, in the 2002 PDG edition [13], $a_2(1990)$ was still listed while the updated states $a_2(1950)$, $a_2(2030)$, $a_2(2175)$, and $a_2(2255)$ were also included [14]. In Ref. [15], the a_2 state with resonance parameters, the mass $M = 2050 \pm 10 \pm 40$ MeV and width $\Gamma = 190 \pm 22 \pm 100$ MeV, was reported in the process $\gamma\gamma \rightarrow \pi^+\pi^-\pi^0$, where this a_2 is considered as the same state as $a_2(2030)$. In addition, the observed a_2 resonance with the mass $2003 \pm 10 \pm 19$ MeV and width $249 \pm 23 \pm 30$ MeV is treated as $a_2(1990)$ since its resonance parameters are close to those of $a_2(1990)$ [16].

Although many a_2 states were reported by experiments, we

notice that these states are not established, especially for the states listed as further states in PDG, which is the main reason why we are interested in the study of the a_2 states. It is obvious that the detailed information on the partial decay widths of the a_2 states is helpful for further experimental study on these. Comparing our theoretical results with the measured resonance parameters, we can further test whether they are suitably categorized into the a_2 meson family. In the next section, we briefly review the possible assignments of the states in the a_2 meson family. Considering the present research status of these states, we notice that a systematic and phenomenological study of the a_2 is still absent. Hence, in this work we carry out the calculation of the Okubo-Zweig-Iizuka (OZI) allowed partial decay widths of these states, where the quark pair creation (QPC) model proposed by Micu [17] will be applied to the whole calculation. The systematical study will give us the valuable partial and total decay widths of the discussed a_2 states in detail.

This paper is organized as follows. In the next section, we briefly introduce different categorizations of the states in the a_2 meson family. Further, we calculate the corresponding two-body OZI-allowed strong decays. After combining the present experimental data with our theoretical results, a phenomenological analysis will be given. The final section is devoted to a summary of our work.

II. MASS SPECTRUM ANALYSIS AND CALCULATION OF TWO-BODY STRONG DECAYS

A. Mass spectrum analysis of the a_2 states

Before calculating the OZI-allowed two-body strong decay widths, we briefly review the status of the mass spectrum analysis of the a_2 states. Usually, the analysis of the Regge trajectories can be an effective approach to study the categorization of mesons. In Refs. [2, 18, 19], Anisovich *et al.* studied the light meson spectrum via the analysis of the Regge trajectories. As indicated in Ref. [2], $a_2(1320)$, $a_2(1700)$, $a_2(1950)$, and $a_2(2175)$ can be assigned to 1^3P_2 , 2^3P_2 , 3^3P_2 , and 4^3P_2 states, respectively, while $a_2(2030)$ and

‡Corresponding author

*Electronic address: pangchq13@lzu.edu.cn

†Electronic address: help08@lzu.edu.cn

§Electronic address: xiangliu@lzu.edu.cn

¶Electronic address: matsuki@tokyo-kasei.ac.jp

TABLE I: The resonance parameters and observed decay channels of the a_2 states collected in PDG [1]. Here, the states listed as further states in PDG are marked by the superscript \ddagger .

State	Mass (MeV)	Width (MeV)	Decay channel
$a_2(1320)$	$1318.3^{+0.5}_{-0.6}$	$105.0^{+1.6}_{-1.9}$	$\pi\rho, \pi\eta, KK, \pi\eta',$ $\pi f_2(1270), \pi\rho(1450)$ [1]
$a_2(1700)$	1732 ± 16	194 ± 40	$\pi\rho, \pi\eta, KK, \pi f_2(1270), \rho\omega$ [1]
$a_2(1950)^\ddagger$	1950^{+30}_{-70}	180^{+30}_{-70}	$\pi f_2(1270)$ [2]
$a_2(1990)^\ddagger$	$2050 \pm 10 \pm 40$	$190 \pm 22 \pm 100$	$\pi\eta, \pi\eta'$ [2, 3]
$a_2(2030)^\ddagger$	2030 ± 20	205 ± 30	$\pi f_2(1270), \pi\eta, \pi\eta'$ [2, 3]
$a_2(2175)^\ddagger$	2175 ± 40	310^{+90}_{-45}	$\pi f_2(1270)$ [2, 3]
$a_2(2255)^\ddagger$	2255 ± 20	230 ± 15	$\pi f_2(1950), \pi\eta$ [2, 3]

TABLE II: Different categorizations of the a_2 meson family. Here, the states with the superscript p are the predicted states in the corresponding analysis.

$n^{2S+1}L_J$	A. Anisovich [2, 3, 20]	V. Anisovich [21, 22]	Masjuan [14]
1^3P_2	$a_2(1320)$	$a_2(1320)$	$a_2(1320)$
2^3P_2	$a_2(1700)$	$a_2(1700)$	$a_2(1700)$
3^3P_2	$a_2(1950)$	$a_2(1950)$	$a_2(2175)$
4^3P_2	$a_2(2175)$	$a_2(2225)$	$a_2(2420)^p$
1^3F_2	$a_2(2030)$	$a_2(2030)$	$a_2(2030)$
2^3F_2	$a_2(2225)$	$a_2(2310)^p$	$a_2(2225)$

$a_2(2255)$ are good candidates for the 1^3F_2 and 2^3F_2 states, respectively [2, 3, 20]. However, in Refs. [21, 22] $a_2(2175)$ was not included in their analysis. Alternatively, $a_2(2255)$ is treated as the 4^3P_2 state and $a_2(2310)$ as the 2^3F_2 state [22]. Recently, Masjuan *et al.* [14] pointed out that $a_2(1950)$ and $a_2(2030)$ might be the same state. Their analysis indicates that $a_2(1320)$, $a_2(1700)$, and $a_2(2175)$ are 1^3P_2 , 2^3P_2 and 3^3P_2 states, respectively. Furthermore, the 4^3P_2 state with the mass 2.42(17) GeV was predicted in their trajectory analysis. The obtained assignments to $a_2(2030)$ and $a_2(2255)$ in Ref. [14] are consistent with those in Ref. [2]. In Table II, we summarize the three different categorizations mentioned above.

B. Brief review of the QPC model

In this work, we study the two-body OZI-allowed strong decays of the a_2 states under the three categorizations. In the following, we briefly explain the QPC model adopted here. After the QPC model [17] was proposed, this model was further developed by the Orsay group of Le Yaouanc *et al.* [23–27]. Later, this model was widely applied to study the OZI-allowed strong decay of hadrons [28–46].

For a two-body strong decay process $A \rightarrow B + C$, the corresponding transition matrix element can be written as

$$\langle BC|T|A\rangle = \delta^3(\mathbf{P}_B + \mathbf{P}_C) \mathcal{M}^{M_{J_A} M_{J_B} M_{J_C}}, \quad (1)$$

where $\mathbf{P}_{B(C)}$ denotes the three-momentum of the final particle $B(C)$. M_{J_i} ($i = A, B, C$) is the orbital magnetic momentum of the corresponding meson in the decay. $\mathcal{M}^{M_{J_A} M_{J_B} M_{J_C}}$ is the helicity amplitude. The T operator reads as

$$T = -3\gamma \sum_m \langle 1m; 1 - m | 00 \rangle \int d\mathbf{p}_3 d\mathbf{p}_4 \delta^3(\mathbf{p}_3 + \mathbf{p}_4) \times \mathcal{Y}_{1m} \left(\frac{\mathbf{p}_3 - \mathbf{p}_4}{2} \right) \chi_{1,-m}^{34} \phi_0^{34} \omega_0^{34} b_{3i}^\dagger(\mathbf{p}_3) d_{4j}^\dagger(\mathbf{p}_4), \quad (2)$$

where γ is a parameter that takes the value 8.7 or $8.7/\sqrt{3}$ depending on whether the quark-antiquark pair created from the vacuum is $u\bar{u}(d\bar{d})$ or $s\bar{s}$ [43]. The quark and antiquark created from the vacuum are marked by the subscripts 3 and 4, respectively. i/j denotes the color indices. The χ , ϕ , and ω are the spin, flavor, and color wave functions, respectively. In addition, $\mathcal{Y}_{lm}(\mathbf{p}) = |\mathbf{p}| Y_{lm}(\mathbf{p})$ is the solid harmonic polynomial (see Refs. [47, 48] for more details). Using the Jacob-Wick formula [49], the helicity amplitude $\mathcal{M}^{M_{J_A} M_{J_B} M_{J_C}}$ can be converted into the partial wave amplitude $M^{JL}(\mathbf{P})$, i.e.,

$$\mathcal{M}^{JL}(\mathbf{P}) = \frac{\sqrt{2L+1}}{2J_A+1} \sum_{M_{J_B} M_{J_C}} \langle L0; JM_{J_A} | J_A M_{J_A} \rangle \times \langle J_B M_{J_B}; J_C M_{J_C} | J_A M_{J_A} \rangle \mathcal{M}^{M_{J_A} M_{J_B} M_{J_C}}. \quad (3)$$

TABLE III: The OZI-allowed two-body decay channels of the discussed a_2 states. Here, ρ , ω , η and η' denote $\rho(770)$, $\omega(782)$, $\eta(548)$, and $\eta'(958)$, respectively. We use \checkmark to mark the allowed decay channels.

channel	$a_2(1320)$	$a_2(1700)$	$a_2(1950)$	$a_2(2030)$	$a_2(2175)$	$a_2(2255)$
$\pi\eta$	\checkmark	\checkmark	\checkmark	\checkmark	\checkmark	\checkmark
$\pi\rho$	\checkmark	\checkmark	\checkmark	\checkmark	\checkmark	\checkmark
KK	\checkmark	\checkmark	\checkmark	\checkmark	\checkmark	\checkmark
$\pi\eta'$	\checkmark	\checkmark	\checkmark	\checkmark	\checkmark	\checkmark
$\pi b_1(1235)$		\checkmark	\checkmark	\checkmark	\checkmark	\checkmark
KK^*		\checkmark	\checkmark	\checkmark	\checkmark	\checkmark
$\pi f_2(1270)$		\checkmark	\checkmark	\checkmark	\checkmark	\checkmark
$\pi f_1(1280)$		\checkmark	\checkmark	\checkmark	\checkmark	\checkmark
$\pi\eta(1295)$		\checkmark	\checkmark	\checkmark	\checkmark	\checkmark
$\rho\omega$		\checkmark	\checkmark	\checkmark	\checkmark	\checkmark
$\pi f_1(1420)$		\checkmark	\checkmark	\checkmark	\checkmark	\checkmark
$\pi\rho(1450)$		\checkmark	\checkmark	\checkmark	\checkmark	\checkmark
$\pi\eta(1475)$		\checkmark	\checkmark	\checkmark	\checkmark	\checkmark
$\pi f_2'(1525)$		\checkmark	\checkmark	\checkmark	\checkmark	\checkmark
$\pi\eta_2(1645)$			\checkmark	\checkmark	\checkmark	\checkmark
$KK_1(1270)$			\checkmark	\checkmark	\checkmark	\checkmark
$\eta a_1(1260)$			\checkmark	\checkmark	\checkmark	\checkmark
K^*K^*			\checkmark	\checkmark	\checkmark	\checkmark
$\pi\rho_3(1690)$			\checkmark	\checkmark	\checkmark	\checkmark
$\pi\eta(1300)$			\checkmark	\checkmark	\checkmark	\checkmark
$\pi\rho(1700)$			\checkmark	\checkmark	\checkmark	\checkmark
$\eta a_2(1320)$			\checkmark	\checkmark	\checkmark	\checkmark
$KK_1(1400)$			\checkmark	\checkmark	\checkmark	\checkmark
$KK^*(1410)$			\checkmark	\checkmark	\checkmark	\checkmark
$KK_2^*(1430)$			\checkmark	\checkmark	\checkmark	\checkmark
$\rho h_1(1170)$			\checkmark	\checkmark	\checkmark	\checkmark
$\rho a_1(1260)$				\checkmark	\checkmark	\checkmark
$\omega b_1(1230)$				\checkmark	\checkmark	\checkmark
$\pi\rho(1900)$				\checkmark	\checkmark	\checkmark
$\rho\pi(1300)$					\checkmark	\checkmark
$\rho a_2(1320)$					\checkmark	\checkmark
$\pi f_2(2010)$					\checkmark	\checkmark
$\pi f_4(2050)$					\checkmark	\checkmark
$K^*K_1(1270)$					\checkmark	\checkmark
$\eta' a_1(1260)$						\checkmark
$\rho\omega(1420)$						\checkmark
$KK^*(1680)$						\checkmark
$\eta\pi_2(1670)$						\checkmark
$\omega\rho(1450)$						\checkmark
$\rho a_0(1450)$						\checkmark

Finally, the decay width can be given by

$$\Gamma = \pi^2 \frac{|\mathbf{P}|}{m_A^2} \sum_{J,L} |\mathcal{M}^{JL}(\mathbf{P})|^2, \quad (4)$$

where m_A is the mass of the initial meson A . In the concrete calculation, we use the harmonic oscillator wave function to

describe the meson spacial wave function, where we approximately take the harmonic oscillator potential to describe the potential between quark and antiquark [50]. The harmonic oscillator wave function has the following expression:

$$\Psi_{nlm}(R, \mathbf{p}) = \mathcal{R}_{nl}(R, \mathbf{p}) \mathcal{Y}_{lm}(\mathbf{p}), \quad (5)$$

where R is a parameter, which is given in Ref. [33] for the mesons involved in our calculation.

The two-body OZI-allowed strong decay channels, which are allowed by the conservation law and calculated by us, are listed in Table III for $a_2(1320)$, $a_2(1700)$, $a_2(1950)$, $a_2(2175)$, $a_2(2030)$, and $a_2(2255)$.

C. Phenomenological analysis of two-body decays

1. $a_2(1320)$, $a_2(1700)$, and $a_2(2030)$

From Table II, we notice that different groups obtained the consistent conclusion of the assignments to $a_2(1320)$, $a_2(1700)$, and $a_2(2030)$, which are the 1^3P_2 , 2^3P_2 , and 1^3F_2 states, respectively. In the following, we discuss the decay behaviors of $a_2(1320)$, $a_2(1700)$, and $a_2(2030)$.

As for $a_2(1320)$, there are four allowed decay channels. We present the dependence of total and partial decay widths on the R value in Fig. 1, and compare the obtained total decay width with the experimental data. The calculated total decay width of $a_2(1320)$ is consistent with the experimental data measured by Ref. [51] when taking $R = 3.85 \text{ GeV}^{-1}$ [33]. Our result also shows that $\pi\rho$ is the dominant decay mode and $\pi\eta$ is another main decay mode. Since there is the abundant experimental information on $a_2(1320)$, we list the comparison between theoretical and experimental results of five typical ratios and two partial decay widths in Table IV, which indicates that our calculation is comparable with the present experimental data. Thus, $a_2(1320)$ as the 1^3P_2 state is well tested by our study.

From PDG [1], we also notice there were the measurement results of $a_2(1320) \rightarrow \omega\pi\pi$ and $a_2(1320) \rightarrow 3\pi$, where the breaching ratios of $a_2(1320) \rightarrow \omega\pi\pi$ and $a_2(1320) \rightarrow 3\pi$ can reach up to $(70.1 \pm 2.7)\%$ and $(10.6 \pm 3.2)\%$, respectively. This information also stimulates our interest in investigating these three-body decays. The two-body decay behavior of $a_2(1320)$ indicates that the $\pi\rho$ channel is its dominant decay mode, where ρ dominantly decays into 2π [branching ratios $\mathcal{B}(\rho \rightarrow \pi\pi) \sim 100\%$]. In addition, the 2π in $a_2(1320) \rightarrow \omega\pi\pi$ can be from the intermediate ρ . Thus, we consider $a_2(1320) \rightarrow \pi\rho \rightarrow 3\pi$ and $a_2(1320) \rightarrow \omega\rho\omega\pi\pi$ processes, where the decay amplitudes of $a_2(1320) \rightarrow \pi\rho$ and $a_2(1320) \rightarrow \omega\rho$ can be obtained by the QPC model. And then we apply the general expressions for three-body decays, i.e.,

$$\Gamma_{A \rightarrow B+C \rightarrow 1+2+C} = \int_{m_1+m_2}^{m_A-m_3} \frac{dE}{2\pi} \frac{\Gamma_{A \rightarrow B+C} \Gamma_{B \rightarrow 1+2}}{(E - m_B)^2 + \Gamma_B^2/4}, \quad (6)$$

where Γ_B is the total width of meson B and E is the energy of particle B . By the calculation, finally we obtain $\Gamma_{a_2(1320) \rightarrow 3\pi} \approx$

90 MeV and $\Gamma_{a_2(1320) \rightarrow \omega \pi^+ \pi^-} \simeq 15$ MeV, which are comparable with the corresponding experimental data [1].

In addition, $a_2(1320) \rightarrow \pi^\pm \gamma$ can from $a_2(1320) \rightarrow \pi^\pm \rho \rightarrow \pi^\pm \gamma$ when one considers the Vector-Meson-Dominance mechanism. Since in this work we only focus on the strong decays, we do not discuss the $a_2(1320) \rightarrow \pi^\pm \gamma$ radiative decay.

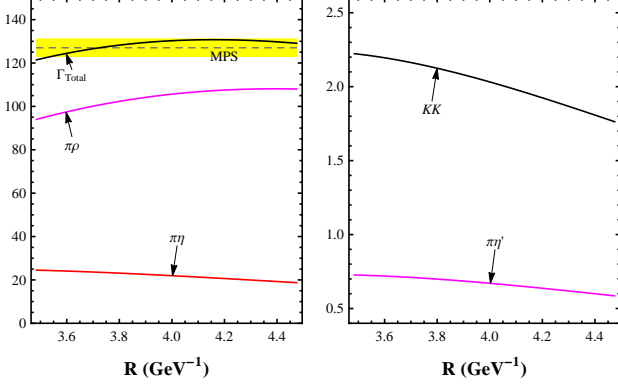


FIG. 1: The partial and total decay widths of $a_2(1320)$ as the 1^3P_2 state dependent on the R value. Here, the dashed line with the yellow band is the experimental total width from Ref. [51]. All results are in units of MeV.

TABLE IV: The comparison between the calculated results and the experimental data for $a_2(1320)$. $\Gamma_{\pi\eta}$ and Γ_{KK} are in units of MeV.

	This work	Experimental data
$\Gamma_{\pi\eta}/\Gamma_{Total}$	0.18	(0.15 ± 0.04) [52]
$\Gamma_{KK}/\Gamma_{Total}$	0.016	(0.049 ± 0.008) [1]
$\Gamma_{\pi\eta'}/\Gamma_{Total}$	5.4×10^{-3}	$(5.3 \pm 0.9) \times 10^{-3}$ [1]
$\Gamma_{KK}/\Gamma_{\pi\eta}$	0.092	0.08 ± 0.02 [1, 53]
$\Gamma_{\pi\eta'}/\Gamma_{\pi\eta}$	0.030	0.032 ± 0.009 [1, 54]
$\Gamma_{\pi\eta}$	23	18.5 ± 3.0 [1, 55]
Γ_{KK}	2.1	$7.0^{+2.0}_{-1.5}$ [1, 55]

As for $a_2(1700)$, more decay channels open as shown in Table II. In Fig. 2 we list the variation of the total and partial decay widths of $a_2(1700)$ in terms of the R value. When $R = 4.35$ GeV^{-1} [33], the central value of the experimental total width of $a_2(1700)$ from L3 [56] can be reproduced by our calculation. The main decay modes of $a_2(1700)$ include $\pi\rho$, $\rho\omega$, $\pi\eta$, and $\pi b_1(1235)$. Additionally, $\pi f_1(1285)$, $\pi\eta'$, $\pi\eta'(1295)$, $\pi\rho(1450)$, and KK are important decay channels for $a_2(1700)$. In Table V, further theoretical values of Γ_{Total} , $\Gamma_{\pi\eta}$, Γ_{KK} and $\Gamma_{\pi\rho}/\Gamma_{\pi f_2(1270)}$ are presented by making the comparison with the corresponding experimental results, where most theoretical values are consistent with the experimental data if one considers the experimental errors. The above study supports $a_2(1700)$ as a 2^3P_2 state in the a_2 meson family.

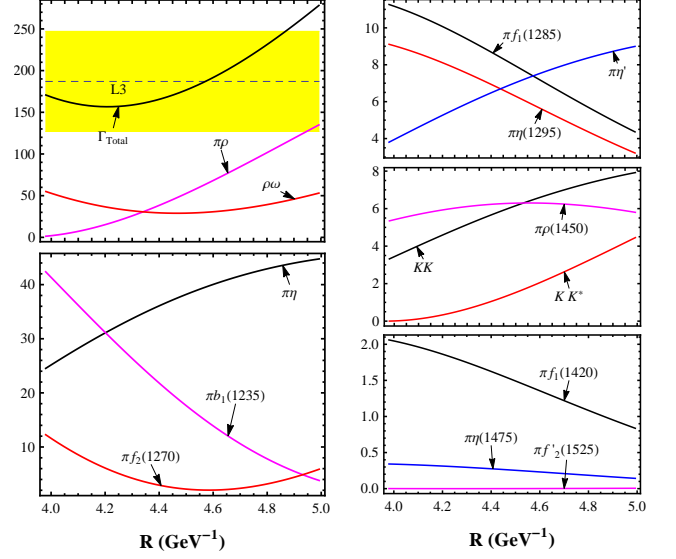


FIG. 2: The dependence of the partial and total decay widths of $a_2(1700)$ as the 2^3P_2 state on the R value. Here, the dashed line with the yellow band denotes the experimental total width given in Ref. [56]. All results are in units of MeV.

TABLE V: The comparison of the theoretical and experimental values for $a_2(1700)$. Here, Γ_{Total} , $\Gamma_{\pi\eta}$, Γ_{KK} are in units of MeV.

Item	This work	Experimental data
Γ_{Total}	161	194 ± 40 [1]
$\Gamma_{\pi\eta}$	35	9.5 ± 2.0 [1, 55]
Γ_{KK}	5.4	5.0 ± 3.0 [1, 55]
$\Gamma_{\pi\rho}/\Gamma_{\pi f_2(1270)}$	8.4	$3.4 \pm 0.4 \pm 0.1$ [1, 15]

Along with investigating the decay behaviors of $a_2(1320)$ and $a_2(1700)$, the reliability of the QPC model can be further tested in this work, which makes us safely apply this model to the remaining a_2 states.

In the following, we illustrate the decay behavior of $a_2(2030)$ as a 1^3F_2 state, where its total and partial decay widths are shown in Fig. 3. Our calculation shows that $a_2(2030)$ as a 1^3F_2 state has a very broad width, i.e., the total width can reach up to (730~830) MeV corresponding to $R = (4.00 \sim 5.00)$ GeV^{-1} , which is not strongly dependent on the R value. When comparing the calculated total width with the experimental result, we find that the theoretical result is far larger than the experimental width of $a_2(2030)$ [2]. At present, $a_2(2030)$ was only reported in Ref. [2, 15]. Thus, we suggest further experimental study to measure the resonance parameters of $a_2(2030)$, which is important to clarify the difference between theory and experiment. From Fig. 3, we obtain that $\pi b_1(1235)$, $\rho h_1(1170)$, $\pi\eta_2(1645)$, $\eta a_1(1260)$, and $\pi f_2(1270)$ are main decay modes of $a_2(2030)$, where $\pi f_2(1270)$ was al-

ready observed in the Crystal Barrel experiments [2, 3, 20]. The details of other decay information of $a_2(2030)$ can be found in Fig. 3. The predicted decay behaviors of $a_2(2030)$ are valuable to confirm this state by future experiments.

2. The possibility of $a_2(1950)$ or $a_2(2175)$ as the 3^3P_2 state

As shown in Table II, there are two possible candidates for the 3^3P_2 state, i.e., $a_2(1950)$ and $a_2(2175)$. Thus, the study of the decay behaviors of $a_2(1950)$ and $a_2(2175)$ is helpful to distinguish these two possibilities. In Table III, the allowed decay channels of $a_2(1950)$ and $a_2(2175)$ are listed. In the following calculation, we separately discuss the decay behaviors of $a_2(1950)$ and $a_2(2175)$ under the 3^3P_2 assignment.

In Fig. 4, we show the total and partial decay widths of $a_2(1950)$ dependent on the R value. Here, the calculated total width overlaps with the SPEC experimental data [2] with $R = (4.73 \sim 5.14) \text{ GeV}^{-1}$. The result of the corresponding partial decay width shows that $a_2(1950)$ dominantly decays into $\pi\rho$, $\pi\eta$, $\rho\omega$, and $\pi\eta'$ (see Fig. 4 for more details). In addition, we also select some typical ratios in Table VI that are weakly dependent on the R values.

TABLE VI: The typical ratios relevant to the decay behavior of $a_2(1950)$. Here, these results correspond to the range $R = (4.73 \sim 5.14) \text{ GeV}^{-1}$.

Ratios	Value	Ratios	Value
$\Gamma_{\pi\rho}/\Gamma_{Total}$	0.229~0.364	$\Gamma_{\pi\eta}/\Gamma_{Total}$	0.200~0.285
$\Gamma_{\rho\omega}/\Gamma_{Total}$	0.0613~0.0763	$\Gamma_{\rho\omega}/\Gamma_{\pi\rho}$	0.210~0.267
$\Gamma_{\rho\omega}/\Gamma_{\pi\eta}$	0.215~0.381	$\Gamma_{\pi\eta'}/\Gamma_{Total}$	0.0520~0.0663
$\Gamma_{\pi\eta'}/\Gamma_{\pi\eta}$	0.233~0.260	$\Gamma_{\pi\eta'}/\Gamma_{\rho\omega}$	0.681~1.08
$\Gamma_{\pi b_1(1235)}/\Gamma_{\pi\eta}$	0.229~0.333	$\Gamma_{\pi b_1(1235)}/\Gamma_{\pi\eta'}$	0.881~1.43
$\Gamma_{KK}/\Gamma_{Total}$	0.0360~0.0449	$\Gamma_{KK}/\Gamma_{\pi\eta}$	0.158~0.180
$\Gamma_{KK}/\Gamma_{\rho\omega}$	0.472~0.732	$\Gamma_{KK}/\Gamma_{\pi\eta'}$	0.676~0.692
$\Gamma_{KK}/\Gamma_{\pi\eta(1295)}$	0.796~0.897	$\Gamma_{KK}/\Gamma_{\pi f_1(1285)}$	0.735~1.03

If $a_2(2175)$ is the 3^3P_2 state, the obtained total decay width can be fitted with the present experimental width of $a_2(2175)$ when taking $R = (4.20 \sim 4.72) \text{ GeV}^{-1}$. Thus, its partial decay behavior is crucial when we want to distinguish $a_2(1950)$ and $a_2(2175)$ as the 3^3P_2 state. Here, we get that the main decay channels of $a_2(2175)$ are $\pi\rho$, $\rho a_2(1320)$, and $\pi\eta$. The detailed decay information of $a_2(2175)$ is collected in Fig. 5. By this study, we can see that the partial decay behavior of $a_2(2175)$ is indeed different from that of $a_2(1950)$. In particular, there are slight differences in the corresponding typical ratios listed in Tables VI and VII. We expect further experimental study on $a_2(1950)$ and $a_2(2175)$ to confirm these theoretical results in future.

TABLE VII: The typical ratios relevant to the decay behavior of $a_2(2175)$ as the 3^3P_2 or a 4^3P_2 state, where we take $R = (4.20 \sim 4.72)$ and $(5.46 \sim 5.78) \text{ GeV}^{-1}$ corresponding to the 3^3P_2 and 4^3P_2 states, respectively.

Ratios	3P state	4P state
$\Gamma_{\pi\rho}/\Gamma_{Total}$	0.0483~0.289	0.350~0.377
$\Gamma_{\pi\eta}/\Gamma_{Total}$	0.107~0.164	0.140~0.180
$\Gamma_{\pi b_1(1235)}/\Gamma_{Total}$	0.0443~0.0704	0.0345~0.0503
$\Gamma_{\pi b_1(1235)}/\Gamma_{\pi\rho}$	0.226~0.915	0.0885~0.144
$\Gamma_{\pi b_1(1235)}/\Gamma_{\pi\eta}$	0.413~0.431	0.246~0.279
$\Gamma_{\rho\omega}/\Gamma_{Total}$	0.0423~0.0693	0.0294~0.0396
$\Gamma_{\rho\omega}/\Gamma_{\pi\rho}$	0.146~1.27	0.0840~0.105
$\Gamma_{\rho\omega}/\Gamma_{\pi\eta}$	0.268~0.570	0.163~0.282
$\Gamma_{\rho\omega}/\Gamma_{\pi b_1(1235)}$	0.648~1.38	0.585~1.15
$\Gamma_{KK}/\Gamma_{Total}$	0.0147~0.0285	0.0283~0.0332
$\Gamma_{KK}/\Gamma_{\pi\rho}$	0.0984~0.304	0.0750~0.0947
$\Gamma_{KK}/\Gamma_{\pi\eta}$	0.137~0.180	0.184~0.202
$\Gamma_{KK}/\Gamma_{\pi b_1(1235)}$	0.331~0.436	0.659~0.821
$\Gamma_{KK}/\Gamma_{\rho\omega}$	0.240~0.673	0.715~1.14
$\Gamma_{KK}/\Gamma_{\pi\eta'}$	0.525~0.577	0.582~0.602

3. The possibility of $a_2(2175)$ or $a_2(2255)$ as the 4^3P_2 state

The mass spectrum analysis [2, 21] shows that both $a_2(2175)$ and $a_2(2255)$ can be the candidates of the 4^3P_2 state. In the following discussion, we combine the experimental data with the calculated result to predict the partial decay width of $a_2(2175)$ and $a_2(2255)$ under the assignment of the 4^3P_2 state.

If $a_2(2175)$ is the 4^3P_2 state, we find that the obtained total decay width can reproduce the experimental data in Ref. [2], where the R range is taken as $(5.46 \sim 5.78) \text{ GeV}^{-1}$. The corresponding partial decay widths are also listed in Fig. 6, which shows that $\pi\rho$ and $\pi\eta$ are main decay modes. Further giving more abundant information to future experiments, we also collect the typical ratios weakly dependent on the R value in Table VII.

Similarly, we also get the total and partial decay widths of $a_2(2255)$ as the 4^3P_2 state, which are shown in Fig. 7. The main decay modes of $a_2(2255)$ as the 4^3P_2 state are $\pi\rho$ and $\pi\eta$. In Table VIII, we predict some typical ratios, which can test the 4^3P_2 state assignment to $a_2(2255)$ in future experiments.

4. $a_2(2255)$ as the 2^3F_2 state

Finally, we need to discuss the possibility of $a_2(2225)$ as the 2^3F_2 state by studying decay behavior. The comparison between the calculated total decay width and the experimental one of $a_2(2255)$ is shown in Fig. 8, which shows that the experimental data cannot be reproduced, i.e., our result is larger

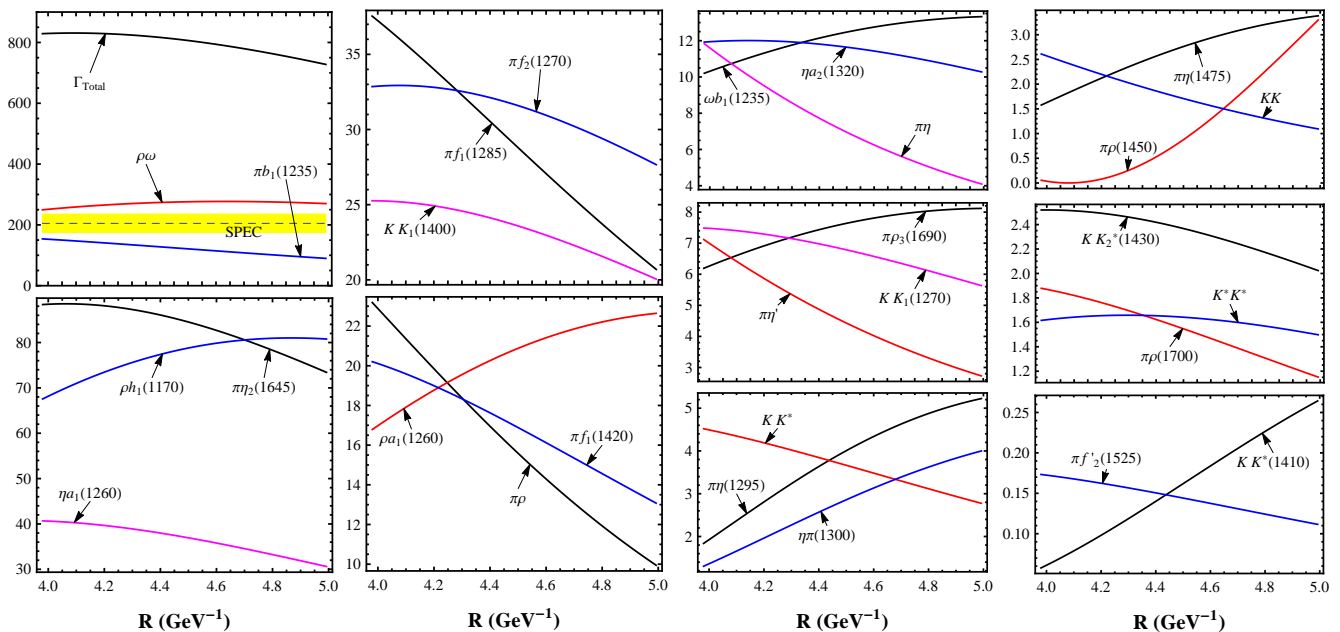


FIG. 3: The variation of the partial and total decay widths of $a_2(2030)$ as a 1^3F_2 state in the R value. Here, the dashed line with the yellow band is the experimental total width from Ref. [2]. All results are in units of MeV.

than the experimental value. There are two possibilities for this:

1. The 2^3F_2 assignment to $a_2(2255)$ is not suitable. However, before definitely adopting this conclusion, a more precise measurement of the resonance parameters of $a_2(2255)$ is necessary since there is only one experiment relevant to $a_2(2255)$ [2] at present.

2. If $a_2(2255)$ is a 2^3F_2 state, the corresponding partial decay widths are listed in Fig. 8. Here, $\rho\omega$ and $\rho a_1(1260)$ are main decay channels. Thus, carrying out the search for these predicted main decay modes will be helpful to clarify whether $a_2(2255)$ as the 2^3F_2 state is suitable or not.

III. SUMMARY

In this work, we have systematically calculated the two-body OZI-allowed strong decays of the observed a_2 states when they are categorized into the a_2 meson family. By comparing our results with the present experimental data, the $n^{2S+1}L_J$ assignments to the observed states can be tested. What is more important is that in this work we have predicted the partial decay widths of the a_2 states, which provides

important and valuable information on further experimental searches for the a_2 states.

As indicated in the review of the experimental status of the a_2 states in Sec. I, the experimental data of these states are not abundant at present, especially the a_2 states with higher mass. Hopefully our work can inspire the experimentalist's interest in exploring the a_2 states. We also suggest future experiments to measure the resonance parameters of the observed a_2 states since these parameters are crucial to establish the a_2 meson family.

The BESIII experiment and the forthcoming PANDA experiment will be good platforms to carry out the experimental study of a_2 , and we expect further experimental progress on the a_2 states.

Acknowledgments

This project is supported by the National Natural Science Foundation of China under Grants No. 11222547, No. 11175073 and No. 11035006, the Ministry of Education of China (SRFDP) under Grant No. 2012021111000, and the Fok Ying Tung Education Foundation (Grant No. 131006).

[1] J. Beringer *et al.* [Particle Data Group Collaboration], Phys. Rev. D **86**, 010001 (2012).

[2] A. V. Anisovich, C. A. Baker, C. J. Batty, D. V. Bugg,

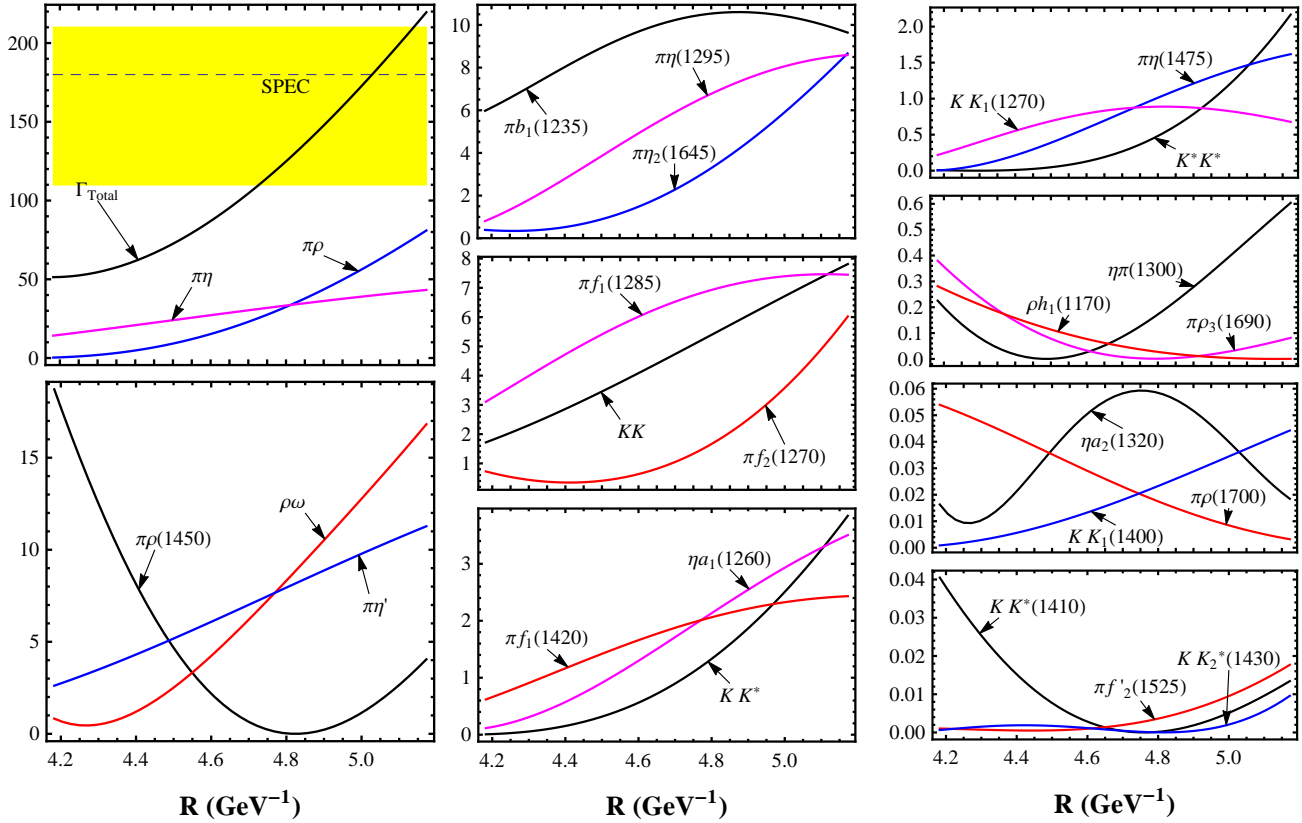


FIG. 4: The dependence of the partial and total decay widths of $a_2(1950)$ as the 3^3P_2 state on the R value. Here, the dashed line with the yellow band is the experimental total width from Ref. [2]. All results are in units of MeV.

- V. A. Nikonov, A. V. Sarantsev, V. V. Sarantsev and B. S. Zou, Phys. Lett. B **517**, 261 (2001) [arXiv:1110.0278 [hep-ex]].
- [3] D. V. Bugg, Phys. Rept. **397**, 257 (2004) [hep-ex/0412045].
- [4] C. Caso *et al.* [Particle Data Group Collaboration], Eur. Phys. J. C **3**, 1 (1998).
- [5] L. Burakovsky and P. R. Page, Eur. Phys. J. C **12**, 489 (2000) [hep-ph/9906282].
- [6] J. D. Anderson, M. H. Austern and R. N. Cahn, Phys. Rev. D **43**, 2094 (1991).
- [7] E. S. Ackleh and T. Barnes, Phys. Rev. D **45**, 232 (1992).
- [8] C. R. Munz, Nucl. Phys. A **609**, 364 (1996) [hep-ph/9601206].
- [9] T. Barnes, F. E. Close, P. R. Page and E. S. Swanson, Phys. Rev. D **55**, 4157 (1997) [hep-ph/9609339].
- [10] C. Amsler *et al.* [Particle Data Group Collaboration], Phys. Lett. B **667**, 1 (2008).
- [11] A. V. Anisovich, C. A. Baker, C. J. Batty, D. V. Bugg, V. A. Nikonov, A. V. Sarantsev, V. V. Sarantsev and B. S. Zou, Phys. Lett. B **517**, 273 (2001) [arXiv:1109.6817 [hep-ex]].
- [12] A. V. Anisovich *et al.* [Crystal Barrel Collaboration], Phys. Lett. B **452**, 173 (1999).
- [13] K. Hagiwara *et al.* [Particle Data Group Collaboration], Phys. Rev. D **66**, 010001 (2002).
- [14] P. Masjuan, E. R. Arriola and W. Broniowski, Phys. Rev. D **85**, 094006 (2012) [arXiv:1203.4782 [hep-ph]].
- [15] V. A. Shchegelsky, A. V. Sarantsev, A. V. Anisovich and M. P. Levchenko, Eur. Phys. J. A **27**, 199 (2006).
- [16] M. Lu *et al.* [E852 Collaboration], Phys. Rev. Lett. **94**, 032002 (2005) [hep-ex/0405044].
- [17] L. Micu, Nucl. Phys. B **10**, 521 (1969).
- [18] A. V. Anisovich *et al.* [Crystal Barrel Collaboration], Phys. Lett. B **452**, 187 (1999).
- [19] A. V. Anisovich, V. V. Anisovich and A. V. Sarantsev, Phys. Rev. D **62**, 051502 (2000) [hep-ph/0003113].
- [20] D. V. Bugg, Phys. Rev. D **87**, no. 11, 118501 (2013) [arXiv:1209.3481 [hep-ph]].
- [21] V. V. Anisovich, Usp. Fiz. Nauk **47**, 49 (2004) [Sov. Phys. Usp. **47**, 45 (2004)] [hep-ph/0208123].
- [22] V. V. Anisovich, AIP Conf. Proc. **717**, 441 (2004) [hep-

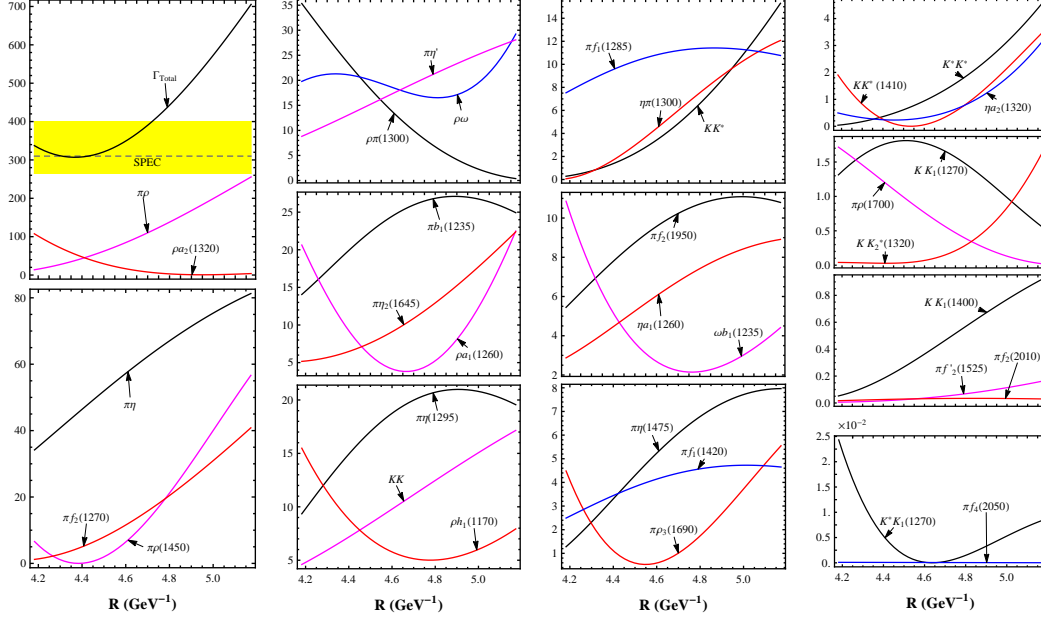


FIG. 5: The decay behavior of $a_2(2175)$ as a 3^3P_2 state. Here, the dashed line with the yellow band is the experimental total width given in Ref. [2]. All results are in units of MeV.

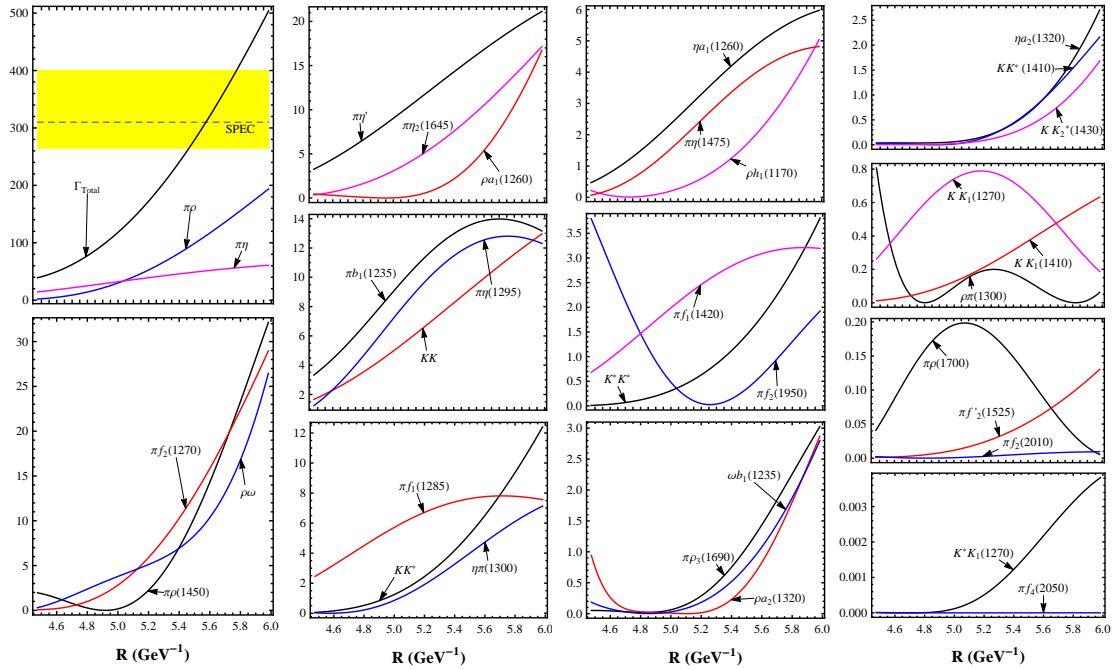


FIG. 6: The obtained total and partial decay widths of $a_2(2175)$ as a 4^3P_2 state on the R value. Here, the dashed line with the yellow band is the experimental total width in Ref. [2]. All results are in units of MeV.

TABLE VIII: The typical ratios relevant to the decay behavior of $a_2(2255)$ as the 4^3P_2 state. Here, these results correspond to the range $R = (5.09 \sim 5.16) \text{ GeV}^{-1}$.

Ratios	Value	Ratios	Value
$\Gamma_{\pi\rho}/\Gamma_{\text{Total}}$	0.300~0.314	$\Gamma_{\pi\eta}/\Gamma_{\text{Total}}$	0.195~0.209
$\Gamma_{\pi\eta}/\Gamma_{\pi\rho}$	0.620~0.696	$\Gamma_{\pi b_1(1235)}/\Gamma_{\text{Total}}$	0.0651~0.0690
$\Gamma_{\pi b_1(1235)}/\Gamma_{\pi\rho}$	0.207~0.2300	$\Gamma_{\pi b_1(1235)}/\Gamma_{\pi\eta}$	0.330~0.334
$\Gamma_{\pi\eta'}/\Gamma_{\text{Total}}$	0.0623~0.0655	$\Gamma_{\pi\eta'}/\Gamma_{\pi\rho}$	0.198~0.218
$\Gamma_{\pi\eta'}/\Gamma_{\pi\eta}$	0.314~0.320	$\Gamma_{\pi\eta'}/\Gamma_{\pi b_1(1235)}$	0.949~0.957
$\Gamma_{\pi\eta(1295)}/\Gamma_{\text{Total}}$	0.0532~0.0565	$\Gamma_{\pi\eta(1295)}/\Gamma_{\pi\rho}$	0.169~0.188
$\Gamma_{\pi\eta(1295)}/\Gamma_{\pi\eta}$	0.271~0.273	$\Gamma_{\pi\eta(1295)}/\Gamma_{\pi b_1(1235)}$	0.817~0.819
$\Gamma_{\pi\eta(1295)}/\Gamma_{\pi\eta'}$	0.854~0.863	$\Gamma_{\pi f_2(1270)}/\Gamma_{\text{Total}}$	0.0408~0.0443
$\Gamma_{\pi f_2(1270)}/\Gamma_{\pi\rho}$	0.136~0.141	$\Gamma_{\pi f_2(1270)}/\Gamma_{\pi\eta}$	0.195~0.228
$\Gamma_{\pi f_2(1270)}/\Gamma_{\pi b_1(1235)}$	0.591~0.681	$\Gamma_{\pi f_2(1270)}/\Gamma_{\pi\eta'}$	0.623~0.712
$\Gamma_{\pi f_2(1270)}/\Gamma_{\pi\eta(1295)}$	0.722~0.834	$\Gamma_{KK}/\Gamma_{\text{Total}}$	0.0335~0.0349
$\Gamma_{KK}/\Gamma_{\pi\rho}$	0.107~0.116	$\Gamma_{KK}/\Gamma_{\pi\eta}$	0.167~0.172
$\Gamma_{KK}/\Gamma_{\pi b_1(1235)}$	0.505~0.515	$\Gamma_{KK}/\Gamma_{\pi\eta'}$	0.532~0.538
$\Gamma_{KK}/\Gamma_{\pi\eta(1295)}$	0.617~0.631	$\Gamma_{KK}/\Gamma_{\pi f_2(1270)}$	0.756~0.855
$\Gamma_{\pi f_1(1285)}/\Gamma_{\text{Total}}$	0.0313~0.0342	$\Gamma_{\pi f_1(1285)}/\Gamma_{\pi\rho}$	0.0996~0.114
$\Gamma_{\pi f_1(1285)}/\Gamma_{\pi\eta}$	0.161~0.164	$\Gamma_{\pi f_1(1285)}/\Gamma_{\pi b_1(1235)}$	0.481~0.496
$\Gamma_{\pi f_1(1285)}/\Gamma_{\pi\eta'}$	0.502~0.522	$\Gamma_{\pi f_1(1285)}/\Gamma_{\pi\eta(1295)}$	0.589~0.605
$\Gamma_{\pi f_1(1285)}/\Gamma_{\pi f_2(1270)}$	0.705~0.839	$\Gamma_{\pi f_1(1285)}/\Gamma_{KK}$	0.933~0.982
$\Gamma_{\pi\rho(1450)}/\Gamma_{\text{Total}}$	0.0201~0.0275	$\Gamma_{\pi\rho(1450)}/\Gamma_{\pi\rho}$	0.0669~0.0875
$\Gamma_{\pi\rho(1450)}/\Gamma_{\pi\eta}$	0.0962~0.141	$\Gamma_{\pi\rho(1450)}/\Gamma_{\pi b_1(1235)}$	0.291~0.422
$\Gamma_{\pi\rho(1450)}/\Gamma_{\pi\eta'}$	0.307~0.441	$\Gamma_{\pi\rho(1450)}/\Gamma_{\pi\eta(1295)}$	0.355~0.517
$\Gamma_{\pi\rho(1450)}/\Gamma_{\pi f_2(1270)}$	0.493~0.619	$\Gamma_{\pi\rho(1450)}/\Gamma_{KK}$	0.576~0.819
$\Gamma_{\pi\rho(1450)}/\Gamma_{\pi f_1(1285)}$	0.587~0.878	$\Gamma_{\pi\eta_2(1645)}/\Gamma_{\text{Total}}$	0.0268~0.0272
$\Gamma_{\pi\eta_2(1645)}/\Gamma_{\pi\rho}$	0.0868~0.0893	$\Gamma_{\pi\eta_2(1645)}/\Gamma_{\pi\eta}$	0.128~0.140
$\Gamma_{\pi\eta_2(1645)}/\Gamma_{\pi b_1(1235)}$	0.388~0.419	$\Gamma_{\pi\eta_2(1645)}/\Gamma_{\pi\eta'}$	0.409~0.438
$\Gamma_{\pi\eta_2(1645)}/\Gamma_{\pi\eta(1295)}$	0.474~0.513	$\Gamma_{\pi\eta_2(1645)}/\Gamma_{\pi f_2(1270)}$	0.614~0.657
$\Gamma_{\pi\eta_2(1645)}/\Gamma_{KK}$	0.769~0.813	$\Gamma_{\pi\eta_2(1645)}/\Gamma_{\pi f_1(1285)}$	0.784~0.871
$\Gamma_{\pi\eta_2(1645)}/\Gamma_{\pi\rho(1450)}$	0.992~1.33	$\Gamma_{\rho\omega}/\Gamma_{\text{Total}}$	0.0217~0.0225
$\Gamma_{\rho\omega}/\Gamma_{\pi\rho}$	0.0693~0.0751	$\Gamma_{\rho\omega}/\Gamma_{\pi\eta}$	0.108~0.112
$\Gamma_{\rho\omega}/\Gamma_{\pi b_1(1235)}$	0.327~0.334	$\Gamma_{\rho\omega}/\Gamma_{\pi\eta'}$	0.344~0.349
$\Gamma_{\rho\omega}/\Gamma_{\pi\eta(1295)}$	0.399~0.409	$\Gamma_{\rho\omega}/\Gamma_{\pi f_2(1270)}$	0.490~0.553
$\Gamma_{\rho\omega}/\Gamma_{KK}$	0.645~0.649	$\Gamma_{\rho\omega}/\Gamma_{\pi f_1(1285)}$	0.659~0.695
$\Gamma_{\rho\omega}/\Gamma_{\pi\rho(1450)}$	0.792~1.12	$\Gamma_{\rho\omega}/\Gamma_{\pi\eta_2(1645)}$	0.798~0.841

- ph/0310165].
- [23] A. Le Yaouanc, L. Oliver, O. Pene and J. C. Raynal, Phys. Rev. D **8**, 2223 (1973).
- [24] A. Le Yaouanc, L. Oliver, O. Pene and J. -C. Raynal, Phys. Rev. D **9**, 1415 (1974).
- [25] A. Le Yaouanc, L. Oliver, O. Pene and J. C. Raynal, Phys. Rev. D **11**, 1272 (1975).
- [26] A. Le Yaouanc, L. Oliver, O. Pene and J. -C. Raynal, Phys. Lett. B **71**, 397 (1977).
- [27] A. Le Yaouanc, L. Oliver, O. Pene and J. C. Raynal, Phys. Lett. B **72**, 57 (1977).
- [28] E. van Beveren, G. Rupp, T. A. Rijken and C. Dullemond, Phys. Rev. D **27**, 1527 (1983).
- [29] S. Capstick and W. Roberts, Phys. Rev. D **49**, 4570 (1994) [nucl-th/9310030].
- [30] H. G. Blundell and S. Godfrey, Phys. Rev. D **53**, 3700 (1996) [hep-ph/9508264].
- [31] E. S. Ackleh, T. Barnes and E. S. Swanson, Phys. Rev. D **54**, 6811 (1996) [hep-ph/9604355].
- [32] S. Capstick and B. D. Keister, [nucl-th/9611055].
- [33] F. E. Close and E. S. Swanson, Phys. Rev. D **72**, 094004 (2005) [hep-ph/0505206].
- [34] B. Zhang, X. Liu, W. -Z. Deng and S. -L. Zhu, Eur. Phys. J. C **50**, 617 (2007) [hep-ph/0609013].
- [35] J. Lu, W. -Z. Deng, X. -L. Chen, and S. -L. Zhu, Phys. Rev. D **73**, 054012 (2006) [hep-ph/0602167].
- [36] Z. -F. Sun and X. Liu, Phys. Rev. D **80**, 074037 (2009) [arXiv:0909.1658 [hep-ph]].
- [37] X. Liu, Z. -G. Luo and Z. -F. Sun, Phys. Rev. Lett. **104**, 122001 (2010) [arXiv:0911.3694 [hep-ph]].
- [38] Z. -F. Sun, J. -S. Yu, X. Liu and T. Matsuki, Phys. Rev. D **82**, 111501 (2010) [arXiv:1008.3120 [hep-ph]].
- [39] T. A. Rijken, M. M. Nagels and Y. Yamamoto, Nucl. Phys. A **835**, 160 (2010).
- [40] J. -S. Yu, Z. -F. Sun, X. Liu and Q. Zhao, Phys. Rev. D **83**, 114007 (2011) [arXiv:1104.3064 [hep-ph]].
- [41] Z. -Y. Zhou and Z. Xiao, Phys. Rev. D **84**, 034023 (2011) [arXiv:1105.6025 [hep-ph]].
- [42] X. Wang, Z. -F. Sun, D. -Y. Chen, X. Liu and T. Matsuki, Phys. Rev. D **85**, 074024 (2012) [arXiv:1202.4139 [hep-ph]].
- [43] Z. -C. Ye, X. Wang, X. Liu and Q. Zhao, Phys. Rev. D **86**, 054025 (2012) [arXiv:1206.0097 [hep-ph]].
- [44] Y. Sun, X. Liu and T. Matsuki, Phys. Rev. D **88**, 094020 (2013) [arXiv:1309.2203 [hep-ph]].
- [45] L. -P. He, X. Wang and X. Liu, Phys. Rev. D **88**, no. 3, 034008 (2013) [arXiv:1306.5562 [hep-ph]].
- [46] Y. Sun, Q. -T. Song, D. -Y. Chen, X. Liu and S. -L. Zhu, Phys. Rev. D **89**, 054026 (2014) [arXiv:1401.1595 [hep-ph]].
- [47] W. Roberts and B. Silvestre-Brac, Acta Phys. Austriaca **11**, 171 (1992).
- [48] H. G. Blundell, hep-ph/9608473.
- [49] M. Jacob and G. C. Wick, Annals Phys. **7**, 404 (1959) [Annals Phys. **281**, 774 (2000)].
- [50] E. van Beveren, Z. Phys. C **17**, 135 (1983) [hep-ph/0602248].
- [51] D. R. Thompson *et al.* [E852 Collaboration], Phys. Rev. Lett. **79**, 1630 (1997) [hep-ex/9705011].
- [52] K. W. J. Barnham, G. S. Abrams, W. R. Butler, D. G. Coyne, G. Goldhaber, B. H. Hall, J. Macnaughton and G. H. Trilling, Phys. Rev. Lett. **26**, 1494 (1971).
- [53] A. Bertin *et al.* [OBELIX Collaboration], Phys. Lett. B **434**, 180 (1998).
- [54] A. Abele *et al.* [Crystal Barrel Collaboration], Phys. Lett. B **404**, 179 (1997).
- [55] V. A. Shchegelsky, A. V. Sarantsev, V. A. Nikonov and A. V. Anisovich, Eur. Phys. J. A **27**, 207 (2006).
- [56] M. Acciarri *et al.* [L3 Collaboration], Phys. Lett. B **501**, 173 (2001) [hep-ex/0011037].